A size-dependent functionally graded sinusoidal plate model based on a modified couple stress theory

Huu-Tai Thai [a,*], Thuc P. Vo [b,c]

[a] Department of Civil and Environmental Engineering, Hanyang University, 17 Haengdang-dong, Seongdong-gu, Seoul 133-791, Republic of Korea

[b] School of Mechanical, Aeronautical and Electrical Engineering, Glyndwr University, Mold Road, Wrexham LL11 2AW, UK.

[c] Advanced Composite Training and Development Centre, Glyndwr University, Unit 5, Hawarden Industrial Park, Deeside, Flintshire CH5 3US, UK.

Abstract

A size-dependent model for bending and free vibration of functionally graded plate is developed based on the modified couple stress theory and sinusoidal shear deformation theory. In the former theory, the small scale effect is taken into consideration, while the effect of shear deformation is accounted for in the latter theory. The equations of motion and boundary conditions are derived from Hamilton's principle. Analytical solutions for the bending and vibration problems of simply supported plates are obtained. Numerical examples are presented to illustrate the influences of small scale on the responses of functionally graded microplates. The results indicate that the inclusion of small scale effects results in an increase in plate stiffness, and consequently, leads to a reduction of deflection and an increase in frequency. Such small scale effects are significant when the plate thickness is small, but become negligible with increasing plate thickness.

Keywords: Functionally graded plate; modified couple stress theory; sinusoidal shear deformation theory; bending; vibration

---

* Corresponding author. Tel.: + 82 2 2220 4154.
E-mail address: thaihuutai@hanyang.ac.kr (H.T. Thai), t.vo@glyndwr.ac.uk (T.P. Vo).

1. Introduction

Functionally graded materials (FGMs) are a class of composites that have continuous variation of material properties from one surface to another and thus eliminate the stress concentration found in laminated composites. Recently, the application of FGMs has broadly been spread in micro- and nano-scale devices and systems such as thin films [1], atomic force microscopes [2], micro- and nano-electro-mechanical systems (MEMS and NEMS) [3]. In such applications, size effects or small scale effects are experimentally observed [4-6]. Conventional plate models based on classical continuum theories do not account for such size effects due to the lack of a material length scale parameter. Thus, needs exist for the development of size-dependent plate models which account for these size effects.

In general, size-dependent plate models can be developed based on size-dependent continuum theories such as classical couple stress theory [7-9], nonlocal elasticity theory [10], and strain gradient theory [11]. In view of the difficulties in determining the material length scale parameters, the modified couple stress theory first proposed by Yang et al. [12] takes an advantage over the aforementioned size-dependent continuum theories due to involving only one material length scale parameter. The modified couple stress theory proposed by Yang et al. [12] results from the classical couple stress theory [7-9]. The two main advantages of the modified couple stress theory over the classical one are the inclusion of asymmetric couple stress tensor and the involvement of only one material length scale parameter. Based on the modified couple stress theory, several size-dependent plate models have been developed. For example, Park and Gao [13] developed Euler-Bernoulli beam model for bending analysis of microbeams. Akgoz and Civalek [14] developed Euler-Bernoulli beam models for buckling analysis of axially loaded microbeams. Ke and Wang [15] developed Timoshenko beam model to study the size effect on dynamic stability of functionally graded (FG) microbeams. Tsiatas [16] developed a size-dependent model for static analysis of microplates using Kirchhoff plate theory (KPT). This model was employed by Yin et al. [17] and Akgoz and Civalek [18] to study the vibration of microplates and nanoplates, respectively. Due to ignoring the shear deformation effect, the KPT provides accurate results for thin homogeneous plates only. For moderately thick FG plates, it underestimates the deflection and overestimates the frequency. Ma et al. [19] and Ke at al. [20] overcome the deficiency of Tsiatas's model by using the first-order shear deformation theory (FSDT) to account for the shear deformation effect. Although the FSDT gives sufficiently accurate result for moderately thick FG plates, it is not convenient to use due to requiring a shear correction factor which is hard to find since it depends on many parameters. To avoid the use of the shear correction factor, Reddy and Kim [21] adopted a higher-order shear deformation theory to develop a size-dependent model for FG microplates.

In general, higher-order shear deformation theories are can be developed based on the higher-order variations of in-plane displacements through the thickness, notable among them are the third-order shear deformation theory of Reddy [22], the sinusoidal shear deformation theory of Touratier [23], the trigonometric shear deformation theory of Ferreira et al. [24], the hyperbolic shear deformation theory of Soldatos [25], and the exponential shear deformation theory of Karama et al. [26]. Among them, the sinusoidal shear deformation theory [23] is widely used because of accuracy and efficiency. Thus, it is adopted herein to develop a size-dependent model for static and free vibration of FG microplates. The aim of this paper is to reformulate the sinusoidal shear deformation theory [23] to account for the small scale effect. The material properties of FG plates are assumed to vary through the thickness according to the power law distribution of the volume fraction of the constituents. The equations of motion and boundary conditions are derived using the modified couple stress theory and Hamilton's principle. Analytical solutions for the bending and vibration problems are obtained for a simply supported plate. Numerical examples are presented to illustrate the influences of small scale on the responses of FG microplates.

2. Theoretical formulation

2.1. Modified couple stress theory

Unlike classical couple stress theory, the modified couple stress theory includes a symmetric couple stress tensor and involves only one length scale parameter. According to the modified couple stress theory, the virtual strain energy can be written as [12]

$$\delta U = \int_V \sigma_{ij} \delta \varepsilon_{ij} dV + \int_V m_{ij} \delta \chi_{ij} dV \tag{1}$$

where summation on repeated indices is implied; σ_{ij} are the components of the stress tensor; ε_{ij} are the components of the strain tensor; m_{ij} are the components of the deviatoric part of the symmetric couple stress tensor; and χ_{ij} are the components of the symmetric curvature tensor defined by

$$\chi_{ij} = \frac{1}{2}\left(\frac{\partial \theta_i}{\partial x_j} + \frac{\partial \theta_j}{\partial x_i} \right), \quad i, j = 1, 2, 3 \tag{2}$$

where θ_i are the components of the rotation vector related to the displacement field (u_1, u_2, u_3) as

$$\theta_x = \theta_1 = \frac{1}{2}\left(\frac{\partial u_3}{\partial x_2} - \frac{\partial u_2}{\partial x_3} \right) \tag{3a}$$

$$\omega_y = \omega_2 = \frac{1}{2}\left(\frac{\partial u_1}{\partial x_3} - \frac{\partial u_3}{\partial x_1}\right) \tag{3b}$$

$$\omega_z = \omega_3 = \frac{1}{2}\left(\frac{\partial u_2}{\partial x_1} - \frac{\partial u_1}{\partial x_2}\right) \tag{3c}$$

2.2. Kinematics

The sinusoidal theory of Touratier [23] is based on the assumption that the transverse shear stress vanishes on the top and bottom surfaces of the plate and is nonzero elsewhere. Thus there is no need to use shear correction factors as in the case of FSDT. According to Touratier [23], the displacement field of sinusoidal theory is given as

$$\begin{aligned} u_1(x,y,z,t) &= u(x,y,t) - z\frac{\partial w}{\partial x} + \frac{h}{\alpha}\sin\left(\frac{\alpha z}{h}\right)\varphi_x \\ u_2(x,y,z,t) &= v(x,y,t) - z\frac{\partial w}{\partial y} + \frac{h}{\alpha}\sin\left(\frac{\alpha z}{h}\right)\varphi_y \\ u_3(x,y,z,t) &= w(x,y,t) \end{aligned} \tag{4}$$

where (u,v,w) are the displacements along the (x,y,z) coordinate directions of a point on the midplane of the plate; φ_x and φ_y are the rotation of the middle surface in the x and y directions, respectively; and h is the plate thickness. The nonzero linear strains of the sinusoidal theory are

$$\varepsilon_{xx} = \frac{\partial u}{\partial x} - z\frac{\partial^2 w}{\partial x^2} + f\frac{\partial \varphi_x}{\partial x} \tag{5a}$$

$$\varepsilon_{yy} = \frac{\partial u}{\partial y} - z\frac{\partial^2 w}{\partial y^2} + f\frac{\partial \varphi_y}{\partial y} \tag{5b}$$

$$\gamma_{xy} = \frac{\partial u}{\partial y} + \frac{\partial v}{\partial x} - 2z\frac{\partial^2 w}{\partial x \partial y} + f\left(\frac{\partial \varphi_x}{\partial y} + \frac{\partial \varphi_y}{\partial x}\right) \tag{5c}$$

$$\gamma_{xz} = g\varphi_x \tag{5d}$$

$$\gamma_{yz} = g\varphi_y \tag{5e}$$

where $f = (h/\pi)\sin(\pi z/h)$, $g = f' = \cos(\pi z/h)$. It can be observed from Eqs. (5d) and (5e) that the transverse shear strains (γ_{xz}, γ_{yz}) are zero at the top ($z = h/2$) and bottom ($z = -h/2$) surfaces of the plate. A shear correction factor is, therefore, not required. Substituting the displacement field (u_1, u_2, u_3) from Eq. (4) into Eq (3), the components of the rotation vector are obtained as

$$\omega_x = \frac{\partial w}{\partial y} - \frac{g}{2}\theta_y \tag{6a}$$

$$\omega_y = -\frac{\partial w}{\partial x} + \frac{g}{2}\theta_x \tag{6b}$$

$$\omega_z = \frac{1}{2}\left(\frac{\partial v}{\partial x} - \frac{\partial u}{\partial y}\right) + \frac{f}{2}\left(\frac{\partial \theta_y}{\partial x} - \frac{\partial \theta_x}{\partial y}\right) \tag{6c}$$

Substituting Eq. (6) into Eq (2), the components of the curvature tensor take the form

$$\chi_{xx} = \frac{\partial^2 w}{\partial x \partial y} - \frac{g}{2}\frac{\partial \theta_y}{\partial x} \tag{7a}$$

$$\chi_{yy} = -\frac{\partial^2 w}{\partial x \partial y} + \frac{g}{2}\frac{\partial \theta_x}{\partial y} \tag{7b}$$

$$\chi_{zz} = \frac{g}{2}\left(\frac{\partial \theta_y}{\partial x} - \frac{\partial \theta_x}{\partial y}\right) \tag{7c}$$

$$\chi_{xy} = \frac{1}{2}\left(\frac{\partial^2 w}{\partial y^2} - \frac{\partial^2 w}{\partial x^2}\right) + \frac{g}{4}\left(\frac{\partial \theta_x}{\partial x} - \frac{\partial \theta_y}{\partial y}\right) \tag{7d}$$

$$\chi_{xz} = \frac{1}{4}\left[\left(\frac{\partial^2 v}{\partial x^2} - \frac{\partial^2 u}{\partial x \partial y}\right) + f\left(\frac{\partial^2 \theta_y}{\partial x^2} - \frac{\partial^2 \theta_x}{\partial x \partial y}\right) + cf\theta_y\right] \tag{7e}$$

$$\chi_{yz} = \frac{1}{4}\left[\left(\frac{\partial^2 v}{\partial x \partial y} - \frac{\partial^2 u}{\partial y^2}\right) + f\left(\frac{\partial^2 \theta_y}{\partial x \partial y} - \frac{\partial^2 \theta_x}{\partial y^2}\right) - cf\theta_x\right] \tag{7f}$$

where $c = (\pi/h)^2$.

2.3. Equations of motion

Hamilton's principle is used herein to derive the equations of motion. The principle can be stated in an analytical form as [27]

$$0=\int_0^T\left(\delta U+\delta W-\delta K\right)dt \tag{8}$$

where δU is the virtual strain energy, δW is the virtual work done by external forces, and δK is the virtual kinetic energy. The virtual strain energy is given by (see Eq. (1))

$$\begin{aligned}
\delta U &= \int_A\int_{-h/2}^{h/2}\left(\sigma_{xx}\delta\varepsilon_{xx}+\sigma_{yy}\delta\varepsilon_{yy}+\sigma_{xy}\delta\gamma_{xy}+\sigma_{xz}\delta\gamma_{xz}+\sigma_{yz}\delta\gamma_{yz}\right)dAdz \\
&+\int_A\int_{-h/2}^{h/2}\left(m_{xx}\delta\chi_{xx}+m_{yy}\delta\chi_{yy}+m_{zz}\delta\chi_{zz}+2m_{xy}\delta\chi_{xy}+2m_{xz}\delta\chi_{xz}+2m_{yz}\delta\chi_{yz}\right)dAdz \\
&=\int_A\left[N_{xx}\frac{\partial\delta u}{\partial x}-M_{xx}\frac{\partial^2\delta w}{\partial x^2}+P_{xx}\frac{\partial\delta\phi_x}{\partial x}+N_{yy}\frac{\partial\delta v}{\partial y}-M_{yy}\frac{\partial^2\delta w}{\partial y^2}+P_{yy}\frac{\partial\delta\phi_y}{\partial y}\right. \\
&\left.+N_{xy}\left(\frac{\partial\delta u}{\partial y}+\frac{\partial\delta v}{\partial x}\right)-2M_{xy}\frac{\partial^2\delta w}{\partial x\partial y}+P_{xy}\left(\frac{\partial\delta\phi_x}{\partial y}+\frac{\partial\delta\phi_y}{\partial x}\right)+Q_{xz}\delta\phi_x+Q_{yz}\delta\phi_y\right]dxdy \\
&+\int_A\left[\left(R_{xx}-R_{yy}\right)\frac{\partial^2\delta w}{\partial x\partial y}+\frac{S_{zz}-S_{xx}}{2}\frac{\partial\delta\phi_y}{\partial x}+\frac{S_{yy}-S_{zz}}{2}\frac{\partial\delta\phi_x}{\partial y}+\frac{c}{2}\left(T_{xz}\delta\phi_y-T_{yz}\delta\phi_x\right)\right. \\
&+R_{xy}\left(\frac{\partial^2\delta w}{\partial y^2}-\frac{\partial^2\delta w}{\partial x^2}\right)+\frac{S_{xy}}{2}\left(\frac{\partial\delta\phi_x}{\partial x}-\frac{\partial\delta\phi_y}{\partial y}\right)+\frac{R_{xz}}{2}\left(\frac{\partial^2\delta v}{\partial x^2}-\frac{\partial^2\delta u}{\partial x\partial y}\right) \\
&\left.+\frac{T_{xz}}{2}\left(\frac{\partial^2\delta\phi_y}{\partial x^2}-\frac{\partial^2\delta\phi_x}{\partial x\partial y}\right)+\frac{R_{yz}}{2}\left(\frac{\partial^2\delta v}{\partial x\partial y}-\frac{\partial^2\delta u}{\partial y^2}\right)+\frac{T_{yz}}{2}\left(\frac{\partial^2\delta\phi_y}{\partial x\partial y}-\frac{\partial^2\delta\phi_x}{\partial y^2}\right)\right]dxdy
\end{aligned} \tag{9}$$

where N, M, P, Q, R, S, and T are the stress resultants defined by

$$\left(N_i,M_i,P_i,Q_i\right)=\int_{-h/2}^{h/2}\left(1,z,f,g\right)\sigma_i dz \tag{10a}$$

$$\left(R_i,S_i,T_i\right)=\int_{-h/2}^{h/2}\left(1,g,f\right)m_i dz \tag{10b}$$

The virtual work done by external forces consists of three parts: (1) virtual work done by the body forces in $V=\Omega\times(-h/2,h/2)$, (2) virtual work done by surface tractions acting on the top and bottom surfaces Ω, and (3) virtual work done by surface tractions acting on the lateral surface $S=\Gamma\times(-h/2,h/2)$, where Ω denotes the middle surface of the plate and Γ is the boundary of the middle surface. Let (f_x, f_y, f_z) be the body forces, (c_x,c_y,c_z) be the body couples, (q_x,q_y,q_z) be the surface forces acting on Ω, and (t_x,t_y,t_z) be the surface forces acting on S. Then, the virtual work done by external forces is [21]

$$\begin{aligned} ¢W=-\Big[\int_\Omega\big(f_x¢u_1+f_y¢u_2+f_z¢u_3+c_x¢¯_x+c_y¢¯_y+c_z¢¯_z\big)dxdy \\ +\int_\Omega\big(q_x¢u_1+q_y¢u_2+q_z¢u_3\big)dxdy+\int_\Gamma\big(t_x¢u_1+t_y¢u_2+t_z¢u_3\big)d\Gamma\Big] \end{aligned} \tag{11}$$

The virtual kinetic energy is expressed as

$$\begin{aligned} ¢K &=\int_V\left(\dot{u}_1¢\dot{u}_1+\dot{u}_2¢\dot{u}_2+\dot{u}_3¢\dot{u}_3\right)°\left(z\right)dAdz \\ &=\int_A\Big[I_0\left(\dot{u}¢\dot{u}+\dot{v}¢\dot{v}+\dot{w}¢\dot{w}\right)+J_1\left(¨_x¢\dot{u}+\dot{u}¢¨_x+¨_y¢\dot{v}+\dot{v}¢¨_y\right) \\ &-I_1\left(\dot{u}\frac{\partial¢\dot{w}}{\partial x}+\frac{\partial\dot{w}}{\partial x}¢\dot{u}+\dot{v}\frac{\partial¢\dot{w}}{\partial y}+\frac{\partial\dot{w}}{\partial y}¢\dot{v}\right)+I_2\left(\frac{\partial\dot{w}}{\partial x}\frac{\partial¢\dot{w}}{\partial x}+\frac{\partial\dot{w}}{\partial y}\frac{\partial¢\dot{w}}{\partial y}\right) \\ &-J_2\left(¨_x\frac{\partial¢\dot{w}}{\partial x}+\frac{\partial\dot{w}}{\partial x}¢¨_x+¨_y\frac{\partial¢\dot{w}}{\partial y}+\frac{\partial\dot{w}}{\partial y}¢¨_y\right)+K_2\left(¨_x¢¨_x+¨_y¢¨_y\right)\Big]dxdy \end{aligned} \tag{12}$$

where dot-superscript convention indicates the differentiation with respect to the time variable t; $°\left(z\right)$ is the mass density; and $\left(I_0,I_1,J_1,I_2,J_2,K_2\right)$ are mass inertias defined by

$$\left(I_0,I_1,J_1,I_2,J_2,K_2\right)=\int_{-h/2}^{h/2}\left(1,z,f,z^2,zf,f^2\right)°\left(z\right)dz \tag{13}$$

Substituting the expressions for $¢U$, $¢V$, and $¢K$ from Eqs. (9), (11), and (12) into Eq. (8) and integrating by parts, and collecting the coefficients of ($¢u,¢v,¢w,¢¨_x,¢¨_y$), the following equations of motion are obtained

$$¢u:\ \frac{\partial N_{xx}}{\partial x}+\frac{\partial N_{xy}}{\partial y}+\frac{1}{2}\left(\frac{\partial^2R_{xz}}{\partial x\partial y}+\frac{\partial^2R_{yz}}{\partial y^2}\right)+f_x+q_x+\frac{1}{2}\frac{\partial c_z}{\partial y}=I_0\ddot{u}-I_1\frac{\partial\ddot{w}}{\partial x}+J_1\dddot{}_x \tag{14a}$$

$$\text{¢}v:\ \frac{\partial N_{xy}}{\partial x}+\frac{\partial N_{yy}}{\partial y}-\frac{1}{2}\left(\frac{\partial^2 R_{xz}}{\partial x^2}+\frac{\partial^2 R_{yz}}{\partial x\partial y}\right)+f_y+q_y-\frac{1}{2}\frac{\partial c_z}{\partial x}=I_0\ddot{v}-I_1\frac{\partial\ddot{w}}{\partial y}+J_1\dddot{\ }_y \tag{14b}$$

$$\begin{aligned}\text{¢}w:&\frac{\partial^2 M_{xx}}{\partial x^2}+2\frac{\partial^2 M_{xy}}{\partial x\partial y}+\frac{\partial^2 M_{yy}}{\partial y^2}+\frac{\partial^2 R_{xy}}{\partial x^2}-\frac{\partial^2 R_{xy}}{\partial y^2}+\frac{\partial^2 (R_{yy}-R_{xx})}{\partial x\partial y}\\&+f_z+q_z+\frac{\partial c_y}{\partial x}-\frac{\partial c_x}{\partial y}=I_0\ddot{w}-I_2\nabla^2\ddot{w}+I_1\left(\frac{\partial\ddot{u}}{\partial x}+\frac{\partial\ddot{v}}{\partial y}\right)+J_2\left(\frac{\partial\dddot{\ }_x}{\partial x}+\frac{\partial\dddot{\ }_y}{\partial y}\right)\end{aligned} \tag{14c}$$

$$\begin{aligned}\text{¢}\ddot{\ }_x:&\ \frac{\partial P_{xx}}{\partial x}+\frac{\partial P_{xy}}{\partial y}-Q_{xz}+\frac{1}{2}\left(\frac{\partial S_{xy}}{\partial x}+\frac{\partial S_{yy}}{\partial y}-\frac{\partial S_{zz}}{\partial y}+\frac{\partial^2 T_{xz}}{\partial x\partial y}+\frac{\partial^2 T_{yz}}{\partial y^2}+cT_{yz}\right)+c_y\frac{h}{\text{®}}\\&=J_1\ddot{u}-J_2\frac{\partial\ddot{w}}{\partial x}+K_2\dddot{\ }_x\end{aligned} \tag{14d}$$

$$\begin{aligned}\text{¢}\ddot{\ }_y:&\ \frac{\partial P_{xy}}{\partial x}+\frac{\partial P_{yy}}{\partial y}-Q_{yz}-\frac{1}{2}\left(\frac{\partial S_{xx}}{\partial x}+\frac{\partial S_{xy}}{\partial y}-\frac{\partial S_{zz}}{\partial x}+\frac{\partial^2 T_{xz}}{\partial x^2}+\frac{\partial^2 T_{yz}}{\partial x\partial y}+cT_{xz}\right)-c_x\frac{h}{\text{®}}\\&=J_1\ddot{v}-J_2\frac{\partial\ddot{w}}{\partial y}+K_2\dddot{\ }_y\end{aligned} \tag{14e}$$

where $\nabla^2=\frac{\partial^2}{\partial x^2}+\frac{\partial^2}{\partial y^2}$ is the Laplacian operator in two-dimensional Cartesian coordinate system. The boundary conditions involve specifying one element of each of the following five pairs:

$$u \text{ or } N_u\equiv N_{xx}n_x+N_{xy}n_y+\frac{1}{2}\left(\frac{\partial R_{xz}}{\partial x}+\frac{\partial R_{yz}}{\partial y}+c_z\right)n_y \tag{15a}$$

$$v \text{ or } N_v\equiv N_{xy}n_x+N_{yy}n_y-\frac{1}{2}\left(\frac{\partial R_{xz}}{\partial x}+\frac{\partial R_{yz}}{\partial y}+c_z\right)n_x \tag{15b}$$

$$\begin{aligned}w \text{ or } V\equiv&\left(\frac{\partial M_{xx}}{\partial x}+\frac{\partial M_{xy}}{\partial y}\right)n_x+\left(\frac{\partial M_{xy}}{\partial x}+\frac{\partial_y M_{yy}}{\partial y}\right)n_y+\left(\frac{\partial R_{xy}}{\partial x}+\frac{\partial R_{yy}}{\partial y}\right)n_x\\&-\left(\frac{\partial R_{xx}}{\partial x}+\frac{\partial R_{xy}}{\partial y}\right)n_y+\left(I_1\ddot{u}+J_2\dddot{\ }_x-I_2\frac{\partial\ddot{w}}{\partial x}\right)n_x+\left(I_1\ddot{v}+J_2\dddot{\ }_y-I_2\frac{\partial\ddot{w}}{\partial y}\right)n_y\end{aligned} \tag{15c}$$

$$\ddot{\ }_x \text{ or } M_{\ddot{\ }x}\equiv P_{xx}n_x+P_{xy}n_y+\frac{1}{2}\left(\frac{\partial T_{xz}}{\partial x}+\frac{\partial T_{yz}}{\partial y}\right)n_y+\frac{1}{2}\left(S_{xy}n_x+S_{yy}n_y-S_{zz}n_y\right) \tag{15d}$$

$$\ddot{}_y \text{ or } M_{\ddot{}y} \equiv P_{xy}n_x + P_{yy}n_y - \frac{1}{2}\left(\frac{\partial T_{xz}}{\partial x} + \frac{\partial T_{yz}}{\partial y}\right)n_x - \frac{1}{2}\left(S_{xy}n_y + S_{xx}n_x - S_{zz}n_x\right) \qquad (15e)$$

where n_x and n_y denote the direction cosines of the unit normal to the boundary of the middle plane.

2.4. Constitutive relations

Consider a FG plate composed of ceramic and metal. The material properties of FG plates such as Young's modulus E and mass density $°$ are assumed to vary continuously through the thickness by a power law as [28]

$$\begin{aligned} E(z) &= E_m + (E_c - E_m)\left(\frac{1}{2}+\frac{z}{h}\right)^p \\ °(z) &= °_m + (°_c - °_m)\left(\frac{1}{2}+\frac{z}{h}\right)^p \end{aligned} \qquad (16)$$

where the subscripts m and c represent the metallic and ceramic constituents, respectively; and p is the power law index. The value of p equal to zero represents a fully ceramic plate, whereas infinite p indicates a fully metallic plate.

The linear elastic constitutive relations are

$$\begin{Bmatrix} \pm_{xx} \\ \pm_{yy} \\ \pm_{xy} \\ \pm_{yz} \\ \pm_{xz} \end{Bmatrix} = \frac{E(z)}{1-\neg^2}\begin{bmatrix} 1 & \neg & 0 & 0 & 0 \\ \neg & 1 & 0 & 0 & 0 \\ 0 & 0 & \frac{(1-\neg)}{2} & 0 & 0 \\ 0 & 0 & 0 & \frac{(1-\neg)}{2} & 0 \\ 0 & 0 & 0 & 0 & \frac{(1-\neg)}{2} \end{bmatrix}\begin{Bmatrix} £_{xx} \\ £_{yy} \\ ¥_{xy} \\ ¥_{yz} \\ ¥_{xz} \end{Bmatrix} \qquad (17a)$$

$$m_{ij} = \frac{E(z)}{1+\neg}\ell^2 ¡_{ij} \qquad (17b)$$

where $\neg$ is the Poisson's ratio assumed to be constant, ℓ is the material length scale parameter which is regarded as a material property measuring the effect of couple stress [29]. This parameter can be determined from torsion tests of slim cylinders [4] or bending tests of thin beams [11]. Substituting Eq. (17) into Eq. (10), the stress resultants can be expressed in terms of generalized displacements $(u, v, w, ¨_x, ¨_y)$ as

$$N_{xx} = A\left(\frac{\partial u}{\partial x} + \neg\frac{\partial v}{\partial y}\right) - B\left(\frac{\partial^2 w}{\partial x^2} + \neg\frac{\partial^2 w}{\partial y^2}\right) + C\left(\frac{\partial ¨_x}{\partial x} + \neg\frac{\partial ¨_y}{\partial y}\right) \quad (18a)$$

$$N_{yy} = A\left(\neg\frac{\partial u}{\partial x} + \frac{\partial v}{\partial y}\right) - B\left(\neg\frac{\partial^2 w}{\partial x^2} + \frac{\partial^2 w}{\partial y^2}\right) + C\left(\neg\frac{\partial ¨_x}{\partial x} + \frac{\partial ¨_y}{\partial y}\right) \quad (18b)$$

$$N_{xy} = A\frac{1-\neg}{2}\left(\frac{\partial u}{\partial y} + \frac{\partial v}{\partial x}\right) - B(1-\neg)\frac{\partial^2 w}{\partial x \partial y} + C\frac{1-\neg}{2}\left(\frac{\partial ¨_x}{\partial y} + \frac{\partial ¨_y}{\partial x}\right) \quad (18c)$$

$$M_{xx} = B\left(\frac{\partial u}{\partial x} + \neg\frac{\partial v}{\partial y}\right) - D\left(\frac{\partial^2 w}{\partial x^2} + \neg\frac{\partial^2 w}{\partial y^2}\right) + F\left(\frac{\partial ¨_x}{\partial x} + \neg\frac{\partial ¨_y}{\partial y}\right) \quad (18d)$$

$$M_{yy} = B\left(\neg\frac{\partial u}{\partial x} + \frac{\partial v}{\partial y}\right) - D\left(\neg\frac{\partial^2 w}{\partial x^2} + \frac{\partial^2 w}{\partial y^2}\right) + F\left(\neg\frac{\partial ¨_x}{\partial x} + \frac{\partial ¨_y}{\partial y}\right) \quad (18e)$$

$$M_{xy} = B\frac{1-\neg}{2}\left(\frac{\partial u}{\partial y} + \frac{\partial v}{\partial x}\right) - D(1-\neg)\frac{\partial^2 w}{\partial x \partial y} + F\frac{1-\neg}{2}\left(\frac{\partial ¨_x}{\partial y} + \frac{\partial ¨_y}{\partial x}\right) \quad (18f)$$

$$P_{xx} = C\left(\frac{\partial u}{\partial x} + \neg\frac{\partial v}{\partial y}\right) - F\left(\frac{\partial^2 w}{\partial x^2} + \neg\frac{\partial^2 w}{\partial y^2}\right) + H\left(\frac{\partial ¨_x}{\partial x} + \neg\frac{\partial ¨_y}{\partial y}\right) \quad (18g)$$

$$P_{yy} = C\left(\neg\frac{\partial u}{\partial x} + \frac{\partial v}{\partial y}\right) - F\left(\neg\frac{\partial^2 w}{\partial x^2} + \frac{\partial^2 w}{\partial y^2}\right) + H\left(\neg\frac{\partial ¨_x}{\partial x} + \frac{\partial ¨_y}{\partial y}\right) \quad (18h)$$

$$P_{xy} = C\frac{1-\neg}{2}\left(\frac{\partial u}{\partial y} + \frac{\partial v}{\partial x}\right) - F(1-\neg)\frac{\partial^2 w}{\partial x \partial y} + H\frac{1-\neg}{2}\left(\frac{\partial ¨_x}{\partial y} + \frac{\partial ¨_y}{\partial x}\right) \quad (18i)$$

$$Q_{xz} = A^s ¨_x, \quad Q_{yz} = A^s ¨_y \quad (18j)$$

$$R_{xx} = 2A_n\frac{\partial^2 w}{\partial x \partial y} - B_n\frac{\partial ¨_y}{\partial x} \quad (18k)$$

$$R_{yy} = -2A_n\frac{\partial^2 w}{\partial x \partial y} + B_n\frac{\partial ¨_x}{\partial y} \quad (18l)$$

$$R_{xy} = A_n\left(\frac{\partial^2 w}{\partial y^2} - \frac{\partial^2 w}{\partial x^2}\right) + \frac{B_n}{2}\left(\frac{\partial ¨_x}{\partial x} - \frac{\partial ¨_y}{\partial y}\right) \quad (18m)$$

$$R_{xz}=\frac{A_n}{2}\left(\frac{\partial^2 v}{\partial x^2}-\frac{\partial^2 u}{\partial x\partial y}\right)+\frac{C_n}{2}\left(\frac{\partial^2\phi_y}{\partial x^2}-\frac{\partial^2\phi_x}{\partial x\partial y}+c\phi_y\right)\tag{18n}$$

$$R_{yz}=\frac{A_n}{2}\left(\frac{\partial^2 v}{\partial x\partial y}-\frac{\partial^2 u}{\partial y^2}\right)+\frac{C_n}{2}\left(\frac{\partial^2\phi_y}{\partial x\partial y}-\frac{\partial^2\phi_x}{\partial y^2}-c\phi_x\right)\tag{18o}$$

$$S_{xx}=2B_n\frac{\partial^2 w}{\partial x\partial y}-D_n\frac{\partial\phi_y}{\partial x}\tag{18p}$$

$$S_{yy}=-2B_n\frac{\partial^2 w}{\partial x\partial y}+D_n\frac{\partial\phi_x}{\partial y}\tag{18q}$$

$$S_{zz}=D_n\left(\frac{\partial\phi_y}{\partial x}-\frac{\partial\phi_x}{\partial y}\right)\tag{18r}$$

$$S_{xy}=B_n\left(\frac{\partial^2 w}{\partial y^2}-\frac{\partial^2 w}{\partial x^2}\right)+\frac{D_n}{2}\left(\frac{\partial\phi_x}{\partial x}-\frac{\partial\phi_y}{\partial y}\right)\tag{18s}$$

$$T_{xz}=\frac{C_n}{2}\left(\frac{\partial^2 v}{\partial x^2}-\frac{\partial^2 u}{\partial x\partial y}\right)+\frac{H_n}{2}\left(\frac{\partial^2\phi_y}{\partial x^2}-\frac{\partial^2\phi_x}{\partial x\partial y}+c\phi_y\right)\tag{18t}$$

$$T_{yz}=\frac{C_n}{2}\left(\frac{\partial^2 v}{\partial x\partial y}-\frac{\partial^2 u}{\partial y^2}\right)+\frac{H_n}{2}\left(\frac{\partial^2\phi_y}{\partial x\partial y}-\frac{\partial^2\phi_x}{\partial y^2}-c\phi_x\right)\tag{18u}$$

where

$$\left(A,B,C,D,F,H\right)=\int_{-h/2}^{h/2}\left(1,z,f,z^2,zf,f^2\right)\frac{E(z)}{1-\nu^2}dz\,,\quad A^s=\int_{-h/2}^{h/2}g^2\frac{E(z)}{2(1+\nu)}dz\tag{19a}$$

$$\left(A_n,B_n,C_n,D_n,H_n\right)=\int_{-h/2}^{h/2}\left(1,g,f,g^2,f^2\right)\frac{\ell^2E(z)}{2(1+\nu)}dz\tag{19b}$$

2.5. Equations of motion in terms of displacements

Substituting Eq. (18) into Eq. (14), the equations of motion can be expressed in terms of generalized displacements (u,v,w,ϕ_x,ϕ_y) as

$$A\left(\frac{\partial^2 u}{\partial x^2}+\frac{1-\nu}{2}\frac{\partial^2 u}{\partial y^2}+\frac{1+\nu}{2}\frac{\partial^2 v}{\partial x\partial y}\right)+\frac{A_n}{4}\nabla^2\left(\frac{\partial^2 v}{\partial x\partial y}-\frac{\partial^2 u}{\partial y^2}\right)-B\nabla^2\frac{\partial w}{\partial x}$$
$$+C\left(\frac{\partial^2 \phi_x}{\partial x^2}+\frac{1-\nu}{2}\frac{\partial^2 \phi_x}{\partial y^2}+\frac{1+\nu}{2}\frac{\partial^2 \phi_y}{\partial x\partial y}\right)+\frac{C_n}{4}\left[\nabla^2\left(\frac{\partial^2 \phi_y}{\partial x\partial y}-\frac{\partial^2 \phi_x}{\partial y^2}\right)+c\left(\frac{\partial^2 \phi_y}{\partial x\partial y}-\frac{\partial^2 \phi_x}{\partial y^2}\right)\right] \quad (20a)$$
$$+f_x+q_x+\frac{1}{2}\frac{\partial c_z}{\partial y}=I_0\ddot{u}-I_1\frac{\partial \ddot{w}}{\partial x}+J_1\ddot{\phi}_x$$

$$A\left(\frac{\partial^2 v}{\partial y^2}+\frac{1-\nu}{2}\frac{\partial^2 v}{\partial x^2}+\frac{1+\nu}{2}\frac{\partial^2 u}{\partial x\partial y}\right)+\frac{A_n}{4}\nabla^2\left(\frac{\partial^2 u}{\partial x\partial y}-\frac{\partial^2 v}{\partial x^2}\right)-B\nabla^2\frac{\partial w}{\partial y}$$
$$+C\left(\frac{\partial^2 \phi_y}{\partial y^2}+\frac{1-\nu}{2}\frac{\partial^2 \phi_y}{\partial x^2}+\frac{1+\nu}{2}\frac{\partial^2 \phi_x}{\partial x\partial y}\right)+\frac{C_n}{4}\left[\nabla^2\left(\frac{\partial^2 \phi_x}{\partial x\partial y}-\frac{\partial^2 \phi_y}{\partial x^2}\right)+c\left(\frac{\partial^2 \phi_x}{\partial x\partial y}-\frac{\partial^2 \phi_y}{\partial x^2}\right)\right] \quad (20b)$$
$$+f_y+q_y-\frac{1}{2}\frac{\partial c_z}{\partial x}=I_0\ddot{v}-I_1\frac{\partial \ddot{w}}{\partial y}+J_1\ddot{\phi}_y$$

$$B\nabla^2\left(\frac{\partial u}{\partial x}+\frac{\partial v}{\partial y}\right)-\left(D+A_n\right)\nabla^4 w+\left(F+\frac{B_n}{2}\right)\nabla^2\left(\frac{\partial \phi_x}{\partial x}+\frac{\partial \phi_y}{\partial y}\right)$$
$$+f_z+q_z+\frac{\partial c_y}{\partial x}-\frac{\partial c_x}{\partial y}=I_0\ddot{w}-I_2\nabla^2\ddot{w}+I_1\left(\frac{\partial \ddot{u}}{\partial x}+\frac{\partial \ddot{v}}{\partial y}\right)+J_2\left(\frac{\partial \ddot{\phi}_x}{\partial x}+\frac{\partial \ddot{\phi}_y}{\partial y}\right) \quad (20c)$$

$$C\left(\frac{\partial^2 u}{\partial x^2}+\frac{1-\nu}{2}\frac{\partial^2 u}{\partial y^2}+\frac{1+\nu}{2}\frac{\partial^2 v}{\partial x\partial y}\right)+\frac{C_n}{4}\left[\nabla^2\left(\frac{\partial^2 v}{\partial x\partial y}-\frac{\partial^2 u}{\partial y^2}\right)+c\left(\frac{\partial^2 v}{\partial x\partial y}-\frac{\partial^2 u}{\partial y^2}\right)\right]$$
$$+H\left(\frac{\partial^2 \phi_x}{\partial x^2}+\frac{1-\nu}{2}\frac{\partial^2 \phi_x}{\partial y^2}+\frac{1+\nu}{2}\frac{\partial^2 \phi_y}{\partial x\partial y}\right)+\frac{H_n}{4}\nabla^2\left[\left(\frac{\partial^2 \phi_y}{\partial x\partial y}-\frac{\partial^2 \phi_x}{\partial y^2}\right)+2c\left(\frac{\partial^2 \phi_y}{\partial x\partial y}-\frac{\partial^2 \phi_x}{\partial y^2}\right)\right] \quad (20d)$$
$$+\frac{D_n}{4}\left(\frac{\partial^2 \phi_x}{\partial x^2}+4\frac{\partial^2 \phi_x}{\partial y^2}-3\frac{\partial^2 \phi_y}{\partial x\partial y}\right)-\left(F+\frac{B_n}{2}\right)\nabla^2\frac{\partial w}{\partial x}-\left(A_s+\frac{c^2 H_n}{4}\right)\phi_x=J_1\ddot{u}-J_2\frac{\partial \ddot{w}}{\partial x}+K_2\ddot{\phi}_x$$

$$C\left(\frac{\partial^2 v}{\partial y^2}+\frac{1-\nu}{2}\frac{\partial^2 v}{\partial x^2}+\frac{1+\nu}{2}\frac{\partial^2 u}{\partial x\partial y}\right)+\frac{C_n}{4}\left[\nabla^2\left(\frac{\partial^2 u}{\partial x\partial y}-\frac{\partial^2 v}{\partial x^2}\right)+c\left(\frac{\partial^2 u}{\partial x\partial y}-\frac{\partial^2 v}{\partial x^2}\right)\right]$$
$$+H\left(\frac{\partial^2 \phi_y}{\partial y^2}+\frac{1-\nu}{2}\frac{\partial^2 \phi_y}{\partial x^2}+\frac{1+\nu}{2}\frac{\partial^2 \phi_x}{\partial x\partial y}\right)+\frac{H_n}{4}\left[\nabla^2\left(\frac{\partial^2 \phi_x}{\partial x\partial y}-\frac{\partial^2 \phi_y}{\partial x^2}\right)+c\left(\frac{\partial^2 \phi_x}{\partial x\partial y}-\frac{\partial^2 \phi_y}{\partial x^2}\right)\right] \quad (20e)$$
$$+\frac{D_n}{4}\left(\frac{\partial^2 \phi_y}{\partial y^2}+4\frac{\partial^2 \phi_y}{\partial x^2}-3\frac{\partial^2 \phi_x}{\partial x\partial y}\right)-\left(F+\frac{B_n}{2}\right)\nabla^2\frac{\partial w}{\partial y}-\left(A_s+\frac{c^2 E_n}{4}\right)\phi_y=J_1\ddot{v}-J_2\frac{\partial \ddot{w}}{\partial y}+K_2\ddot{\phi}_y$$

Clearly, when size effect is neglected ($\ell=0$), the present model recovers the classical sinusoidal theory [30].

2.6. Analytical solutions

Consider a simply supported rectangular plate under a transverse load. Based on the Navier approach, the solutions are assumed as

$$
\begin{aligned}
u(x,y,t) &= \sum_{m=1}^{\infty}\sum_{n=1}^{\infty} U_{mn} \cos\alpha x \sin\beta y\, e^{i\omega t} \\
v(x,y,t) &= \sum_{m=1}^{\infty}\sum_{n=1}^{\infty} V_{mn} \sin\alpha x \cos\beta y\, e^{i\omega t} \\
w(x,y,t) &= \sum_{m=1}^{\infty}\sum_{n=1}^{\infty} W_{mn} \sin\alpha x \sin\beta y\, e^{i\omega t} \\
\varphi_x(x,y,t) &= \sum_{m=1}^{\infty}\sum_{n=1}^{\infty} X_{mn} \cos\alpha x \sin\beta y\, e^{i\omega t} \\
\varphi_y(x,y,t) &= \sum_{m=1}^{\infty}\sum_{n=1}^{\infty} Y_{mn} \sin\alpha x \cos\beta y\, e^{i\omega t}
\end{aligned} \tag{21}
$$

where $i=\sqrt{-1}$, $\alpha = m\pi/a$, $\beta = n\pi/b$, $(U_{mn}, V_{mn}, W_{bmn}, W_{smn})$ are coefficients, and ω is the frequency of vibration. The transverse load q is also expanded in the double-Fourier sine series as

$$
q(x,y) = \sum_{m=1}^{\infty}\sum_{n=1}^{\infty} Q_{mn} \sin\alpha x \sin\beta y \tag{22}
$$

where

$$
Q_{mn} = \frac{4}{ab}\int_0^a\int_0^b q(x,y)\sin\alpha x \sin\beta y\, dxdy = \begin{cases} q_0 & \text{for sinusoidally distributed load} \\ \dfrac{16q_0}{mn\pi^2} & \text{for uniformly distributed load} \end{cases} \tag{23}
$$

Substituting Eqs. (21) and (22) into Eq. (20), the analytical solutions can be obtained from the following equations

$$
\left(\begin{bmatrix} s_{11} & s_{12} & s_{13} & s_{14} & s_{15} \\ s_{12} & s_{22} & s_{23} & s_{24} & s_{25} \\ s_{13} & s_{23} & s_{33} & s_{34} & s_{35} \\ s_{14} & s_{24} & s_{34} & s_{44} & s_{45} \\ s_{15} & s_{25} & s_{35} & s_{45} & s_{55} \end{bmatrix} - \omega^2 \begin{bmatrix} m_{11} & 0 & m_{13} & m_{14} & 0 \\ 0 & m_{22} & m_{23} & 0 & m_{25} \\ m_{13} & m_{23} & m_{33} & m_{34} & m_{35} \\ m_{14} & 0 & m_{34} & m_{44} & 0 \\ 0 & m_{25} & m_{35} & 0 & m_{55} \end{bmatrix} \right) \begin{Bmatrix} U_{mn} \\ V_{mn} \\ W_{mn} \\ X_{mn} \\ Y_{mn} \end{Bmatrix} = \begin{Bmatrix} 0 \\ 0 \\ Q_{mn} \\ 0 \\ 0 \end{Bmatrix} \tag{24}
$$

where

$$s_{11} = A\left(\sim^2 + \tfrac{1-\neg}{2}\;^2\right) + \frac{A_n}{4}\;^2\left(\sim^2 + \;^2\right),\; s_{12} = \tfrac{1+\neg}{2}A\sim \;-\frac{A_n}{4}\sim\;\left(\sim^2 + \;^2\right)$$

$$s_{13} = -B\sim\left(\sim^2 + \;^2\right),\; s_{14} = C\left(\sim^2 + \tfrac{1-\neg}{2}\;^2\right) + \frac{C_n}{4}\;^2\left(\sim^2 + \;^2 - c\right)$$

$$s_{15} = \tfrac{1+\neg}{2}C\sim \;-\frac{C_n}{4}\sim\;\left(\sim^2 + \;^2 - c\right),\; s_{22} = A\left(\;^2 + \tfrac{1-\neg}{2}\sim^2\right) + \frac{A_n}{4}\sim^2\left(\sim^2 + \;^2\right)$$

$$s_{23} = -B\;\left(\sim^2 + \;^2\right),\; s_{24} = s_{15},\; s_{25} = C\left(\;^2 + \tfrac{1-\neg}{2}\sim^2\right) + \frac{C_n}{4}\sim^2\left(\sim^2 + \;^2 - c\right)$$

$$s_{33} = \left(D + A_n\right)\left(\sim^2 + \;^2\right)^2,\; s_{34} = -\left(F + \frac{B_n}{2}\right)\left(\sim^2 + \;^2\right)\sim$$

$$s_{35} = -\left(F + \frac{B_n}{2}\right)\left(\sim^2 + \;^2\right)\;,\; s_{45} = \left[\tfrac{1+\neg}{2}H - \frac{H_n}{4}\left(\sim^2 + \;^2 - 2c\right) - \frac{3D_n}{4}\right]\sim$$

$$s_{44} = A^s + H\left(\sim^2 + \tfrac{1-\neg}{2}\;^2\right) + \frac{H_n}{4}\left[\;^2\left(\sim^2 + \;^2 - 2c\right) + c^2\right] + \frac{D_n}{4}\left(\sim^2 + 4\;^2\right)$$

$$s_{55} = A^s + H\left(\;^2 + \tfrac{1-\neg}{2}\sim^2\right) + \frac{H_n}{4}\left[\sim^2\left(\sim^2 + \;^2 - 2c\right) + c^2\right] + \frac{D_n}{4}\left(4\sim^2 + \;^2\right)$$

$$m_{11} = m_{22} = I_0,\; m_{13} = -\sim I_1,\; m_{14} = J_1,\; m_{23} = -\;I_1,\; m_{25} = J_1$$

$$m_{33} = I_0 + I_2\left(\sim^2 + \;^2\right),\; m_{34} = -\sim J_2,\; m_{35} = -\;J_2,\; m_{44} = m_{55} = K_2 \qquad (25)$$

3. Numerical results

3.1. Verification studies

Since the results of microplate made of FGM are not available in the open literature, only homogeneous microplates ($p = 0$) is used herein for the verification. Table 1 shows the fundamental frequencies of simply supported square plates with various values of side-to-thickness ratio a/h. The microplate is made of epoxy with the following material properties: $E = 1.44$ GPa, $\neg = 0.38$, $\circ = 1220$ kg/m^3, $\ell = 17.6\times10^{-6}$m, and $h = 2\ell$ [20]. The obtained frequencies are compared with those reported by Yin et al. [17] based on the KPT and Ke et al. [20] based on the FSDT. It can be seen that the obtained analytical results are in good agreement with the p-version Ritz solutions of Ke et al. [20] based on the FSDT. The difference between the KPT [17] and shear deformation theories (i.e., FSDT [20] and present model) is observed to be quite small when side-to-thickness ratio $a/h \geq 20$ but relatively large when $a/h < 20$. This is due to the transverse shear deformation effects which are more pronounced in moderately thick and thick plates are included in the shear deformation theories, but neglected in the KPT [17].

3.2. Parameter studies

Parameter studies are presented to investigate the influences of material length scale parameter ℓ and power law index p on the bending and vibration responses of FG microplate. Unless mentioned otherwise, a simply supported square FG microplate with $a/h = 10$ is considered. This plate is composed of aluminum Al (as metal) and alumina Al_2O_3 (as ceramic). Young's modulus and mass density of aluminum are $E_m = 70$ GPa and $\rho_m = 2702$ kg/m^3, respectively, and that of alumina are $E_c = 380$ GPa and $\rho_c = 3800$ kg/m^3, respectively. Poisson's ratio is assumed to be constant through the thickness and equal to 0.3. The material length scale parameter $\ell = 17.6 \times 10^{-6}$ m is based on the experimental work reported by Lam et al. [11]. For convenience, the following dimensionless forms are used:

$$\bar{w} = \frac{10E_c h^3}{q_0 a^4} w\left(\frac{a}{2},\frac{b}{2}\right),\ \bar{\omega} = \omega \frac{a^2}{h}\sqrt{\rho_c / E_c},\ \bar{\sigma}_x(z) = \frac{h}{q_0 a}\sigma_x\left(\frac{a}{2},\frac{b}{2},z\right),$$
$$\bar{\tau}_{xy}(z) = \frac{h}{q_0 a}\tau_{xy}(0,0,z),\ \bar{\tau}_{xz}(z) = \frac{h}{q_0 a}\tau_{xz}\left(0,\frac{b}{2},z\right) \tag{26}$$

Numerical results of dimensionless stresses are presented in Table 2 for different values of dimensionless material length scale parameter ℓ/h and power law index p. The through thickness variation of stresses are plotted in Figs. 1-3 for a FG microplate ($p = 1$). In these figures, the results of both present model ($\ell \neq 0$) and classical model ($\ell = 0$) are presented. It can be observed that the classical model overestimates stresses of microplates (see Table 2 and Figs. 1-3). It is because the classical model ignores the small scale effects which are significant in microplates. The effects of the length scale parameter on deflection $\bar{w}$ and frequency $\bar{\mu}$ are also presented in Figs. 4-6. It can be seen that the effects of length scale parameter are significant when the plate thickness is small especially at the higher modes (see Fig. 6), but become negligible with increasing plate thickness. This means that the size effect is only significant when the thickness of the plate is at the micron scale, which agrees with the general trends observed in experiments.

The effects of the power law index p on the deflection and frequency are presented in Figs. 7 and 8. It can be seen that increasing value of the power law index leads to an increase in the magnitude of deflection (see Fig. 7) and a reduction of the amplitude of frequency (see Fig. 8). This is due to the fact that higher values of power law index correspond to high portion of metal in comparison with the ceramic part. In other words, an increase of the power-law index results in a reduction of elasticity modulus and bending stiffness, which also implies that the plate becomes flexible. Therefore, it leads to an increase in deflection and a reduction of frequency.

4. Conclusions

Based on the modified couple stress theory and sinusoidal shear deformation theory, a size-dependent model is developed for the bending and free vibration of functionally graded plates. The equations of motion and boundary conditions are derived using Hamilton's principle. Analytical solutions for a simply supported plate are obtained. The present models contain one material length scale parameter and can capture the small scale effect, shear deformation effect, and two-constituent material variation through the plate thickness. The present models can also recover the classical sinusoidal plate model by setting the material length scale parameter equal to zero. The numerical results show that the inclusion of the small scale effect will increase stiffness of the plates, and consequently, leads to a reduction of both deflection and stresses and an increase in frequency. The differences in bending and vibration responses predicted by the present model and the classical model are significant when the plate thickness is small, but they are negligible when the plate thickness becomes larger. These predicted trends agree with the size effect at the micron scale observed in experiments.

References

[1] Fu Y, Du H, Zhang S. Functionally graded TiN/TiNi shape memory alloy films. Materials Letters 2003;57(20):2995-2999.

[2] Rahaeifard M, Kahrobaiyan MH, Ahmadian MT. Sensitivity analysis of atomic force microscope cantilever made of functionally graded materials. In: 3rd International Conference on Micro- and Nanosystems 2009;DETC2009-86254:539-544.

[3] Witvrouw A, Mehta A. The use of functionally graded poly-SiGe layers for MEMS applications. Materials Science Forum 2005;492-493:255-260.

[4] Chong ACM, Yang F, Lam DCC, Tong P. Torsion and bending of micron-scaled structures. Journal of Materials Research 2001;16(04):1052-1058.

[5] Fleck NA, Muller GM, Ashby MF, Hutchinson JW. Strain gradient plasticity: theory and experiment. Acta Metallurgica et Materialia 1994;42(2):475-487.

[6] Stolken JS, Evans AG. A microbend test method for measuring the plasticity length scale. Acta Materialia 1998;46(14):5109-5115.

[7] Koiter WT. Couple stresses in the theory of elasticity, I and II. Nederl. Akad. Wetensch. Proc. Ser. B 1964;67:17-44.

[8] Mindlin RD, Tiersten HF. Effects of couple-stresses in linear elasticity. Archive for Rational Mechanics and Analysis 1962;11(1):415-448.

[9] Toupin RA. Elastic materials with couple-stresses. Archive for Rational Mechanics and Analysis 1962;11(1):385-414.

[10] Eringen AC. Nonlocal polar elastic continua. International Journal of Engineering Science 1972;10(1):1-16.

[11] Lam DCC, Yang F, Chong ACM, Wang J, Tong P. Experiments and theory in strain gradient elasticity. Journal of the Mechanics and Physics of Solids 2003;51(8):1477-1508.

[12] Yang F, Chong ACM, Lam DCC, Tong P. Couple stress based strain gradient theory for elasticity. International Journal of Solids and Structures 2002;39(10):2731-2743.

[13] Park SK, Gao XL. Bernoulli–Euler beam model based on a modified couple stress theory. Journal of Micromechanics and Microengineering 2006;16(11):2355-2359.

[14] Akgoz B, Civalek O. Strain gradient elasticity and modified couple stress models for buckling analysis of axially loaded micro-scaled beams. International Journal of Engineering Science 2011;49(11):1268-1280.

[15] Ke LL, Wang YS. Size effect on dynamic stability of functionally graded microbeams based on a modified couple stress theory. Composite Structures 2011;93(2):342-350.

[16] Tsiatas GC. A new Kirchhoff plate model based on a modified couple stress theory. International Journal of Solids and Structures 2009;46(13):2757-2764.

[17] Yin L, Qian Q, Wang L, Xia W. Vibration analysis of microscale plates based on modified couple stress theory. Acta Mechanica Solida Sinica 2010;23(5):386-393.

[18] Akgoz B, Civalek O. Free vibration analysis for single-layered graphene sheets in

an elastic matrix via modified couple stress theory. Materials & Design 2012;42:164-171.

[19] Ma HM, Gao XL, Reddy JN. A non-classical Mindlin plate model based on a modified couple stress theory. Acta Mechanica 2011;220(1-4):217-235.

[20] Ke LL, Wang YS, Yang J, Kitipornchai S. Free vibration of size-dependent Mindlin microplates based on the modified couple stress theory. Journal of Sound and Vibration 2012;331(1):94-106.

[21] Reddy JN, Kim J. A nonlinear modified couple stress-based third-order theory of functionally graded plates. Composite Structures 2012;94(3):1128-1143.

[22] Reddy JN. Analysis of functionally graded plates. International Journal for Numerical Methods in Engineering 2000;47(1-3):663-684.

[23] Touratier M. An efficient standard plate theory. International Journal of Engineering Science 1991;29(8):901-916.

[24] Ferreira AJM, Roque CMC, Jorge RMN. Analysis of composite plates by trigonometric shear deformation theory and multiquadrics. Computers & Structures 2005;83(27):2225-2237.

[25] Soldatos K. A transverse shear deformation theory for homogeneous monoclinic plates. Acta Mechanica 1992;94(3):195-220.

[26] Karama M, Afaq KS, Mistou S. Mechanical behaviour of laminated composite beam by the new multi-layered laminated composite structures model with transverse shear stress continuity. International Journal of Solids and Structures 2003;40(6):1525-1546.

[27] Reddy JN. Energy principles and variational methods in applied mechanics: John Wiley & Sons Inc; 2002.

[28] Reddy JN. Microstructure-dependent couple stress theories of functionally graded beams. Journal of the Mechanics and Physics of Solids 2011;59(11):2382-2399.

[29] Mindlin RD. Influence of couple-stresses on stress concentrations. Experimental Mechanics 1963;3(1):1-7.

[30] Zenkour AM. Generalized shear deformation theory for bending analysis of functionally graded plates. Applied Mathematical Modelling 2006;30(1):67-84.

Figure Captions

Fig. 1. Variation of in-plane normal stress $\bar{\pm}_x$ across the thickness of a square plate ($p = 1$)

Fig. 2. Variation of in-plane shear stress $\bar{\pm}_{xy}$ across the thickness of a square plate ($p = 1$)

Fig. 3. Variation of transverse shear stress $\bar{\pm}_{xz}$ across the thickness of a square plate ($p = 1$)

Fig. 4. Effect of the material length scale parameter ℓ on the deflection $\bar{w}$ of a square plate

Fig. 5. Effect of the material length scale parameter ℓ on the fundamental frequency $\bar{\mu}$ of a square plate

Fig. 6. Effect of the material length scale parameter ℓ on the higher-order frequencies $\bar{\mu}$ of a square plate ($p = 1$)

Fig. 7. Effect of the power law index p on the deflection $\bar{w}$ of a square plate

Fig. 8. Effect of the power law index p on the fundamental frequency $\bar{\mu}$ of a square plate

Table Captions

Table 1. Fundamental frequency (MHz) of a homogeneous square plate ($p = 0$, $h = 2\ell$)

Table 2. Dimensionless stresses of a FG plate

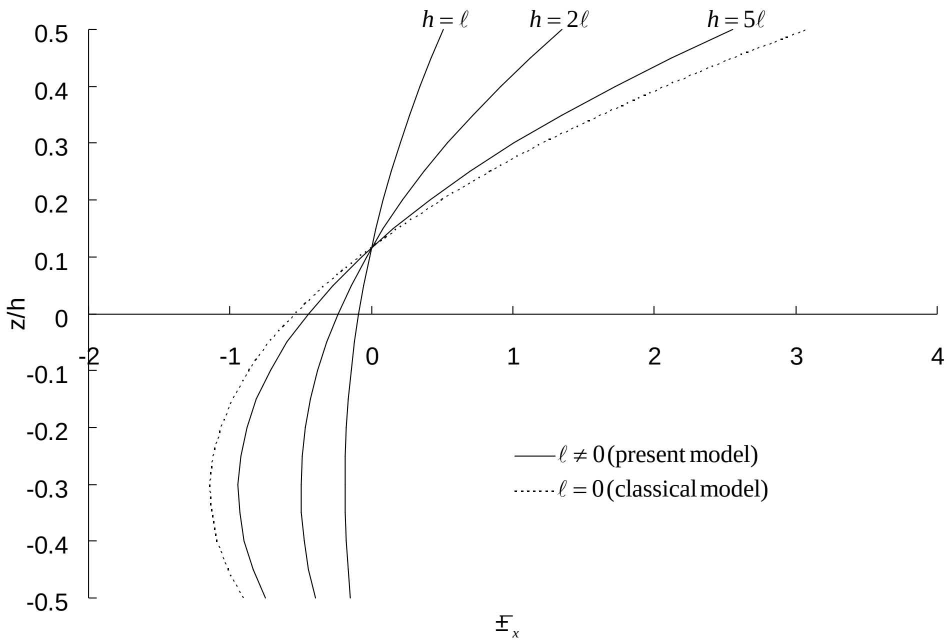

Fig. 1. Variation of in-plane normal stress $\bar{\sigma}_x$ across the thickness of a square plate ($p=1$)

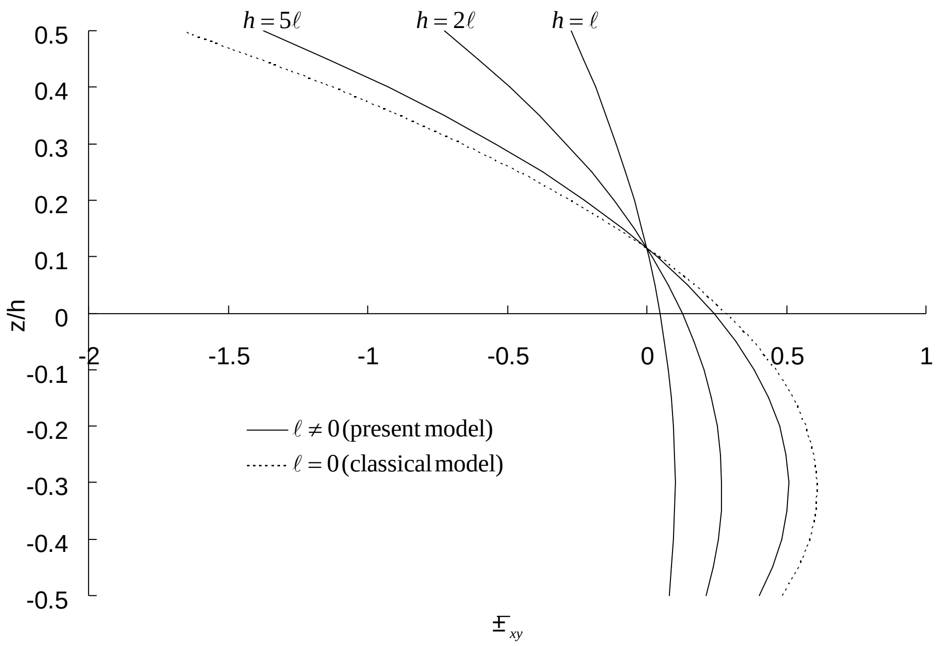

Fig. 2. Variation of in-plane shear stress $\bar{\sigma}_{xy}$ across the thickness of a square plate ($p=1$)

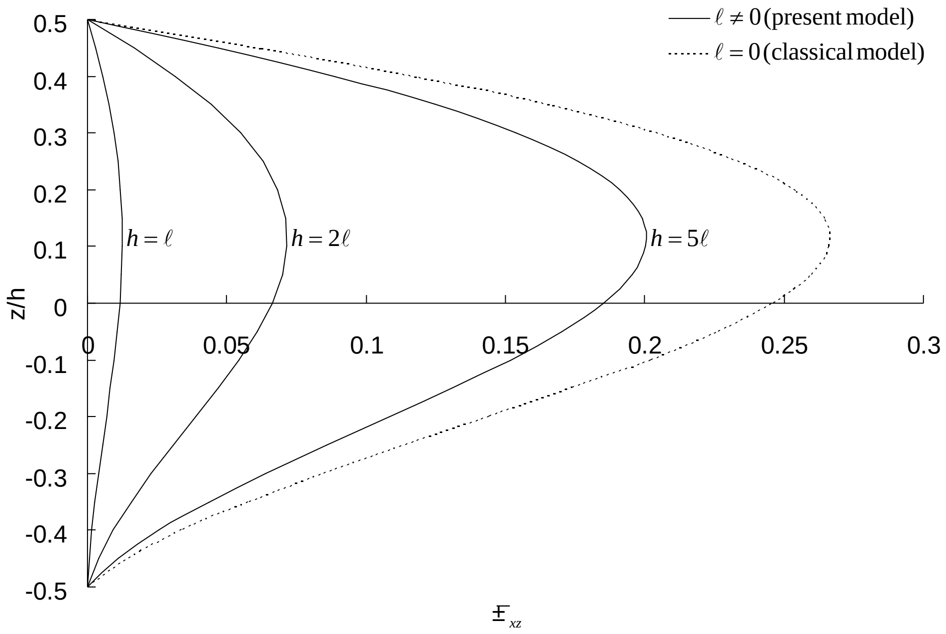

Fig. 3. Variation of transverse shear stress $\pm_{xz}$ across the thickness of a square plate ($p = 1$)

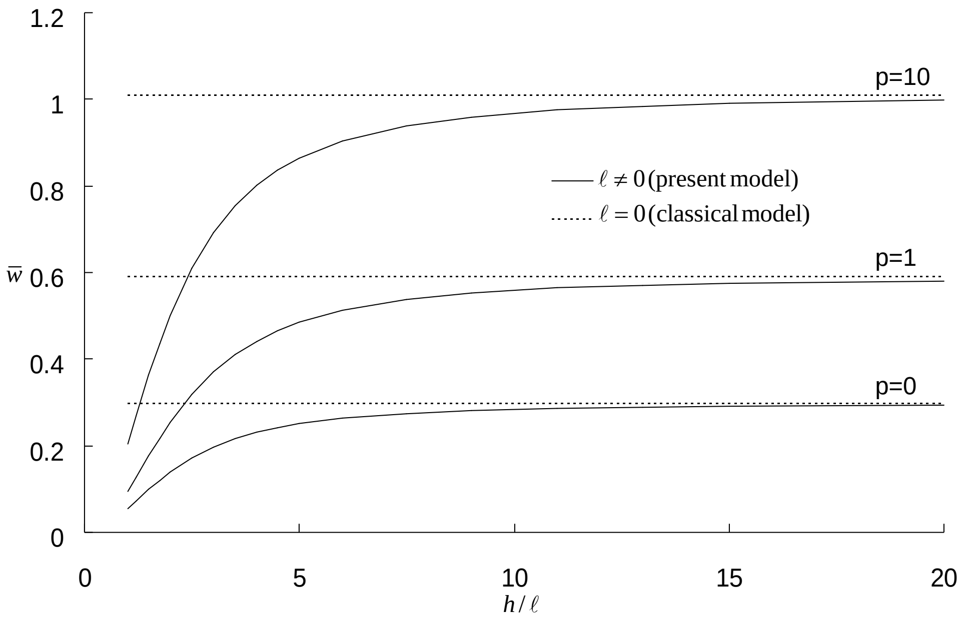

Fig. 4. Effect of the material length scale parameter ℓ on the deflection $\bar{w}$ of a square plate

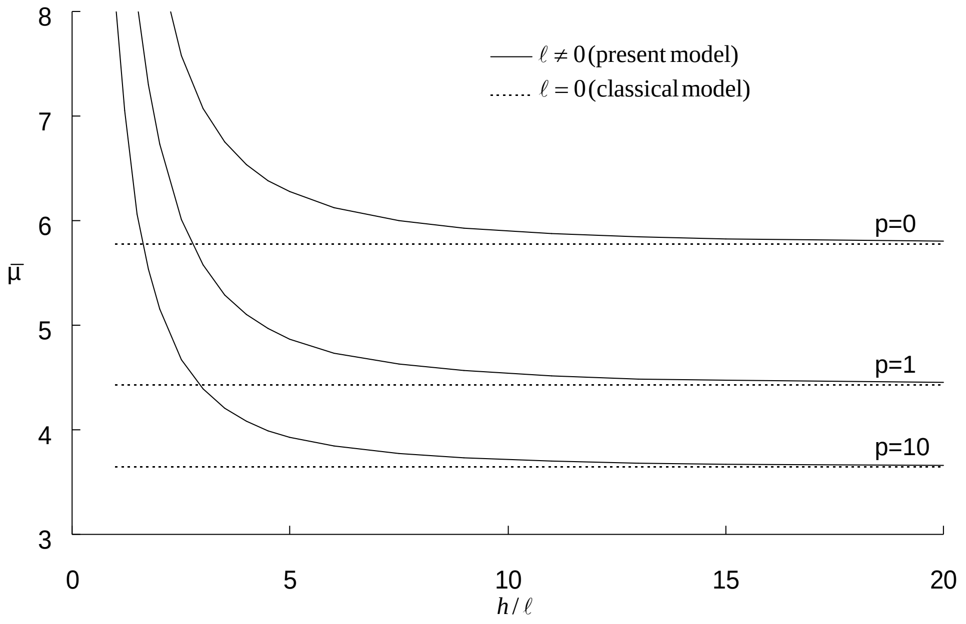

Fig. 5. Effect of the material length scale parameter ℓ on the fundamental frequency $\bar{\mu}$ of a square plate

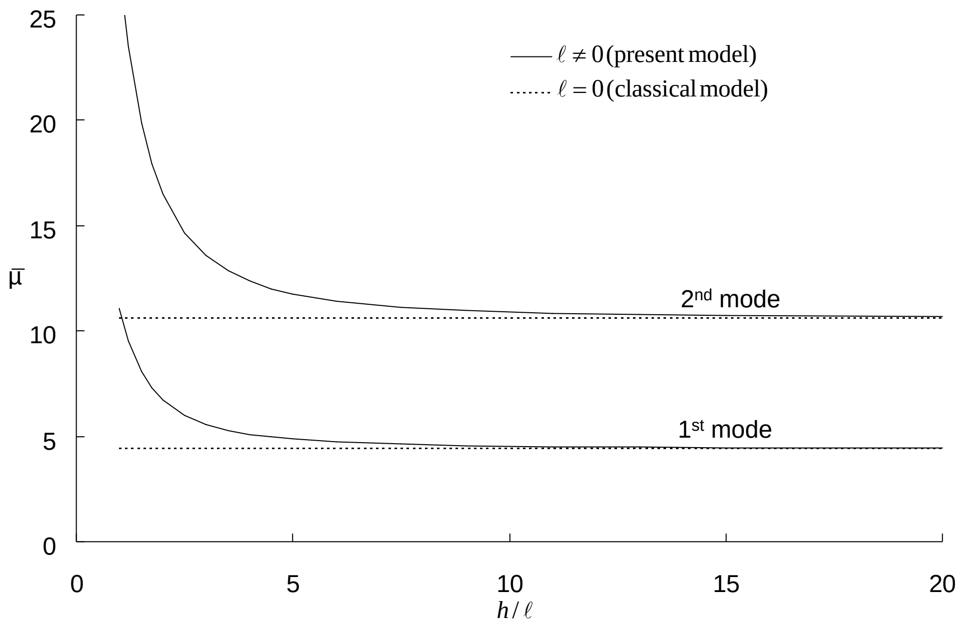

Fig. 6. Effect of the material length scale parameter ℓ on the higher-order frequencies $\bar{\mu}$ of a square plate ($p=1$)

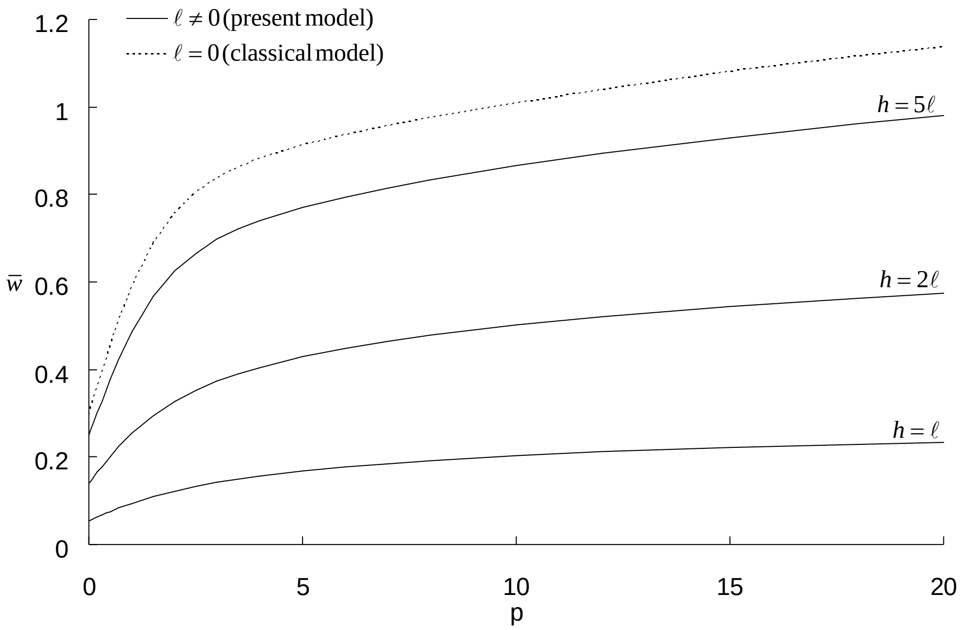

Fig. 7. Effect of the power law index p on the deflection $\bar{w}$ of a square plate

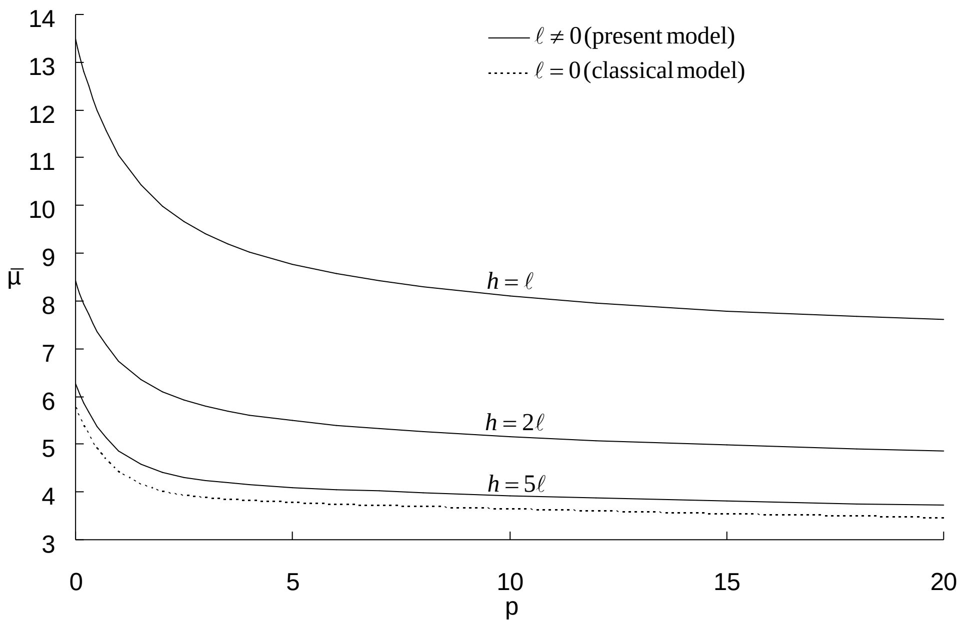

Fig. 8. Effect of the power law index p on the fundamental frequency $\bar{\mu}$ of a square plate

Table 1. Fundamental frequency (MHz) of a homogeneous square plate ($p = 0$, $h = 2\ell$)

a/h	KPT [17]	FSDT [20]	Present
10	0.4204	0.4042	0.4132
20	0.1051	0.1040	0.1046
30	0.0467	0.0465	0.0466

Table 2. Dimensionless stresses of a FG plate

p	ℓ/h	$\bar{\sigma}_x(h/2)$	$\bar{\sigma}_{xy}(-h/3)$	$\bar{\sigma}_{xz}(0)$
0	0	1.9955	0.7065	0.2462
	0.2	1.6945	0.6007	0.1901
	0.5	0.9528	0.3392	0.0725
	1	0.3762	0.1345	0.0133
1	0	3.0870	0.6110	0.2462
	0.2	2.5541	0.5061	0.1881
	0.5	1.3467	0.2677	0.0725
	1	0.5048	0.1007	0.0159
10	0	5.0890	0.5894	0.2198
	0.2	4.4019	0.5111	0.1665
	0.5	2.6050	0.3044	0.0612
	1	1.0737	0.1262	0.0123